Earth and Planetary Science Letters 384 (2013) 198–208

Contents lists available at ScienceDirect

Earth and Planetary Science Letters

www.elsevier.com/locate/epsl

The primary fO_2 of basalts examined by the Spirit rover in Gusev Crater, Mars: Evidence for multiple redox states in the martian interior

Mariek E. Schmidt [a,*], Christian M. Schrader [b,1], Timothy J. McCoy [c]

[a] Department of Earth Sciences, Brock University, Saint Catharines, ON L2S 3A1, Canada
[b] NASA, Marshall Space Flight Center, Huntsville, AL 35813, Unites States
[c] Department of Mineral Sciences, Smithsonian Institution, MRC-0119, PO Box 37012, Washington, DC 20013-7012, United States

ARTICLE INFO

Article history:
Received 24 April 2013
Received in revised form 15 August 2013
Accepted 3 October 2013
Available online 6 November 2013
Editor: T. Elliott

Keywords:
Mars
Gusev basalts
oxygen fugacity
Mössbauer spectrometer

ABSTRACT

The primary oxygen fugacity (fO_2) of basaltic melts reflects the mantle source oxidation state, dictates the crystallizing assemblage, and determines how the magma will evolve. Basalts examined by the Spirit Mars Exploration Rover in Gusev Crater range from the K-poor Adirondack class (0.02 wt% K_2O) to K-rich Backstay class (up to 1.2 wt% K_2O) and exhibit substantially more variation than observed in martian basaltic meteorites. The ratios of ferric to total iron (Fe^{3+}/Fe_T) measured by the Mössbauer spectrometer are high (equivalent to −0.76 to +2.98 ΔQFM; quartz-fayalite-magnetite buffer as defined by Wones and Gilbert, 1969), reflecting secondary Fe^{3+} phases. By combining the Fe^{3+}/Fe_T of the igneous minerals (olivine, pyroxene, and magnetite) determined by Mössbauer spectrometer, we estimate primary fO_2 for the Gusev basalts to be −3.6 to 0.5 ΔQFM. Estimating the fO_2 as a function of the dependence of the CIPW normative fayalite/magnetite ratios on Fe^{3+}/Fe_T yields a slightly smaller range of −2.58 to +0.57ΔQFM. General similarity between the fO_2 estimated for the Gusev basalts and ranges in fO_2 for the shergottitic meteorites (−3.8 to 0.2 ΔQFM; Herd, 2003; Goodrich et al., 2003) suggests that the overall range of fO_2 for the martian igneous rocks and mantle is relatively restricted. Like the shergottites (Herd, 2003), estimated fO_2 of three Gusev classes (Adirondack, Barnhill and Irvine) correlates with a proxy for LREE enrichment (K_2O/TiO_2). This suggests mixing between melts or fluids derived from reservoirs with contrasting fO_2 and REE characteristics. Oxygen fugacity estimates for the martian interior suggest that tectonic processes have not led to sufficient recycling of oxidized surface material into the martian interior to entirely affect the overall oxidation state of the mantle.

1. Introduction

Oxygen fugacity (fO_2) is an important factor in magma petrogenesis because it critically controls mineral stability, depth of the mantle solidus, how the magma may evolve by fractional crystallization, and C–O–H fluid speciation. The distribution of fO_2 in the interior of a planet may further allow insight to planetary differentiation processes, as well as the extent of recycling of surface materials by subduction. As such, the range and distribution of fO_2 in the martian interior is essential for understanding the character and evolution of the planet.

The fO_2 of the martian mantle may be constrained by examining primary mantle melts because in an ideal closed system their fO_2 reflects the oxidation state of the source at the time of extraction. In reality however, fO_2 of basaltic magma may be modified by secondary igneous processes, such as fractional crystallization, crustal assimilation, metasomatism, or degassing. Mixing between melts derived from reduced (mantle) and more oxidized (late-stage fractionated or crustal) reservoirs is thought to be the cause of an increase of up to 3 log unit range in fO_2 among martian shergottite meteorites (Herd, 2003). Differences between early and late crystallizing assemblages for certain shergottites have been interpreted as mixing of reduced and oxidized mantle-derived melts (e.g., NWA 1068/1110; Herd, 2006) or alternatively, oxidation during closed-system crystallization (e.g., LAR 06319; Peslier et al., 2010).

Variable fO_2 among terrestrial primary basalts is linked both to the depth of mantle melting as well as to heterogeneities formed by tectonic processing of the upper mantle. Within the Earth's mantle, fO_2 decreases with depth; the fO_2 of the outer mantle ranges from ~ −0.4 log units relative to the quartz–fayalite–magnetite oxygen buffer (QFM as defined by Wones and Gilbert, 1969) for the MORB source in the upper mantle to ~ −4 log units

* Corresponding author. Tel.: +1 905 688 5550 X3527.
E-mail addresses: mschmidt2@brocku.ca (M.E. Schmidt), Christian.Schrader@ColoradoCollege.edu (C.M. Schrader), mccoyt@si.edu (T.J. McCoy).
[1] Now at: Geology Department, Colorado College, Colorado Springs, CO 80903, United States.

0012-821X/$ – see front matter © 2013 Published by Elsevier B.V.
http://dx.doi.org/10.1016/j.epsl.2013.10.005

relative to QFM for the deepest garnet peridotites from ~6 GPa (Frost and McCammon, 2008). Subarc mantle xenoliths are typically more oxidized, ranging up to +2 log units relative to QFM (Parkinson and Arculus, 1999) – a characteristic likely linked to the mass exchange between the surface and the interior during tectonic processing. The exact process for the oxidation of the subarc mantle wedge is a source of debate and may involve the influx of oxidized sediments and hydrothermal magnetite in the subducted slab or the reduction of sulfate in subduction fluids (e.g., Kelley and Cottrell, 2009; Lécuyer and Ricard, 1999).

The conceptual framework for the distribution of fO_2 in the martian interior is much less developed than for the Earth and for this reason, the martian meteorites are invaluable for detailed determination of magmatic fO_2 conditions. Multiple methods have been employed, including oxybarometry by olivine–pyroxene–spinel or Fe–Ti oxides (e.g., Herd et al., 2001; Herd, 2003; Goodrich et al., 2003), rare earth elements (REE) in augite (Wadhwa, 2001; McCanta et al., 2009) and REE in merrillite–whitlockite (Shearer et al., 2011). The range in fO_2 of basaltic and olivine-phyric shergottites by olivine–pyroxene–spinel oxybarometry, for example, is QFM −3.8 to +0.3 (Herd, 2003, 2006). These microanalytical techniques provide extreme detail for each sample and the results may be interpreted as capturing the fO_2 along a liquid line of descent as other or new techniques are applied (e.g., Goodrich et al., 2003; Peslier et al., 2010). While the advantages to such investigations are clear, the source region for martian meteorites is unknown and they represent a tiny (albeit important) subset of the whole planet.

Relatively unaltered basaltic rocks examined *in situ* by the Spirit Mars Exploration Rover in Gusev Crater represent a complementary dataset to examine the range of fO_2 of the martian interior at an estimated Early Hesperian mantle-extraction age (Greeley et al., 2005). The level of detail for the Gusev basalts is much less than what is known for the SNC meteorites. Even so, whole rock major and minor elemental compositions determined by Alpha Particle X-Ray Spectrometer (APXS; Gellert et al., 2006; Ming et al., 2008) and iron-bearing mineral assemblages determined by Mössbauer spectrometer (Morris et al., 2006a, 2006b, 2008) indicate that the Gusev basalts are a diverse lot. Compositions range from the K-poor Adirondack class (0.02 wt% K_2O) to K-rich Backstay and Humboldt Peak classes (up to 1.2 wt% K_2O). In addition, the Opportunity rover in Meridiani Planum examined one exotic basaltic rock called Bounce Rock that is similar to the basaltic shergottites in major element composition and Fe-bearing mineralogy (Zipfel et al., 2011).

The goal of this paper is to develop methods to estimate the fO_2 of Gusev basalts using a combination of APXS and Mössbauer data. We compare these fO_2 estimates with the SNC meteorites and other planetary systems to make inferences about the distribution of redox states in the martian interior.

2. Basalts examined by the Mars Exploration Rovers

2.1. Gusev basalts

Comparatively unaltered basaltic rocks were first encountered by the Spirit rover in the Gusev Plains and later, in the Columbia Hills. All relatively dust-free surfaces are low albedo with few phenocrysts visible in Microscopic Imager (MI) images. In this paper, we consider four basaltic classes that are distinguished by their elemental compositions. These include: (1) the Adirondack class, which consists of widespread, massive olivine- and pyroxene-bearing angular blocks in the Gusev Plains (McSween et al., 2004); (2) the Backstay class, which includes an apparently aphyric float rock with microphenocrystic olivine, pyroxene, magnetite, and ilmenite as well as other float identified by Mini-TES (Miniature Thermal Emission Spectrometer) on Husband Hill (McSween et al., 2006b); (3) the Irvine class, which includes massive to scoriaceous pyroxene and magnetite-bearing rocks on the flanks of Husband Hill and the Inner Basin of the Columbia Hills (McSween et al., 2006a, 2006b; Schmidt et al., 2008); and (4) the Humboldt Peak class, which includes a pile of olivine-rich rocks just south of the Home Plate outcrop in the Inner Basin. Also, for comparison, we consider the more altered Barnhill class, which includes the layered tephra deposit of Home Plate and is of similar composition to the Irvine class (Schmidt et al., 2008).

For the basaltic classes, the Rock Abrasion Tool (RAT) was only able to abrade surfaces of the Adirondack class rocks before the diamond grinding teeth dulled ~500 sols into the mission (Arvidson et al., 2006). The RAT brush removed dust from surfaces of Backstay, Barnhill, and Humboldt Peak class rocks, but poor positioning of the rover and irregular rock surfaces prevented brushing of Irvine class rocks. It is therefore impossible to completely rule out surface contamination for these classes. RAT-abraded and relatively dust-free surfaces of the targeted basalts were examined by APXS (Rieder et al., 2003). We renormalize the APXS analyses to remove excess volatiles (Cl and >0.3 wt% SO_3) for CIPW norm and fO_2 estimates presented in this paper as has been convention in previous treatments of these data (e.g., McSween et al., 2004). The renormalization affects basalt elemental and oxide abundances by ~1–3% relative.

As a group, the Gusev basalt compositions span a narrower range in MgO (8.3 to 10.8 wt%) than do the shergottite meteorites (5.7 to 33.1 wt%) while having comparable SiO_2 concentrations (Fig. 1). The wide range in MgO of the shergottites is in part caused by olivine accumulation and/or fractionation as is indicated by olivine-phyric and/or cumulate textures in some shergottitic meteorites (McSween and Treiman, 1998). In contrast, the Gusev basalts present little evidence for significant olivine fractionation or accumulation with sparse to no olivine phenocrysts apparent in MI images, a narrow range in MgO, and Ni concentrations of rock interiors in excess of 165 ppm. The total Fe as FeO* concentrations in most Gusev basalts is also generally similar to those of the shergottites. A notable exception to this is the low FeO* rock Backstay, which also has the highest SiO_2 (49.5 wt%) and Al_2O_3 (13.2%) of the Gusev basalts (Fig. 1B).

The greatest elemental variation among the Gusev basalts is in incompatible minor elements, such as K. The unaltered basaltic classes found in the Columbia Hills (Backstay, Irvine, Humboldt Peak) have higher K_2O (Figs. 1A, 2) and total alkalis than do the Adirondack class of the Gusev Plains and the shergottitic meteorites (McSween et al., 2006; Schmidt and McCoy, 2010). The other minor incompatible elements P and Ti (Fig. 2B) are also higher in the Columbia Hills basalts than those examined in the Gusev Plains. The differences in incompatible minor element concentrations have been attributed to fractional crystallization (McSween et al., 2008), but their high Ni concentrations and narrow ranges in MgO suggest fractional crystallization has been minor. Variations in minor elements among the Gusev basalts may also be modeled by multi-stage batch melting of primary martian mantle of Wänke and Dreibus (1988; WD), but with slightly higher K concentrations (Schmidt and McCoy, 2010). If correct, this implies that the martian mantle is heterogeneous and has experienced multiple melt extraction events to form basaltic martian crust. Alternative models for the differences between Gusev basalts may involve mixing between melts derived from enriched and depleted reservoirs, or source metasomatism such as has been suggested for the shergottitic meteorites (e.g., Borg et al., 1997 and Herd et al., 2002). Because fO_2 is more sensitive to mixing between reservoirs than are elemental variations, oxidation state may be an

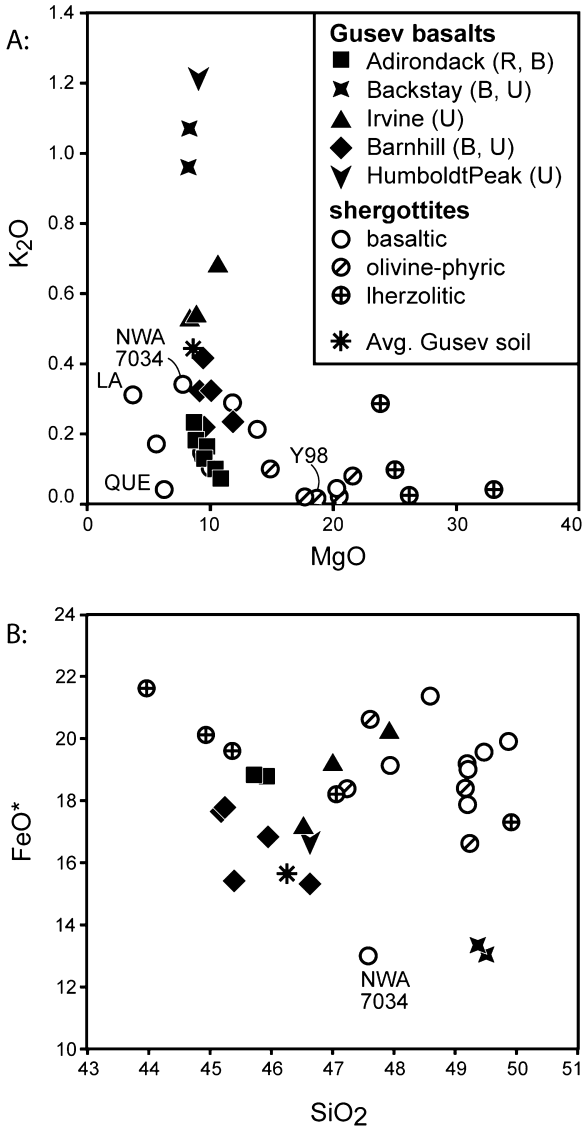

Fig. 1. Elemental variation diagrams for the Gusev basalts and shergottitic meteorites. A. Plot of K_2O vs. MgO illustrates the higher K_2O concentrations of the Columbia Hills basalts (Backstay, Irvine, Barnhill, Humboldt Peak) than the Adirondack basalts and than the meteorites. B Total Fe as FeO* vs. SiO_2. Rock surface types analyzed by the Spirit APXS were RAT abraded (R), RATbrushed (B), or as is (U). Figure is modified from Schmidt and McCoy (2010) and includes additional SNC data from Gross et al. (2011) and Agee et al. (2013a). Select meteorites are indicated (abbreviated LA = Los Angeles, Y98 = Y980459, and QUE = QUE 94201).

important discriminator between these petrogenic models for the Gusev basalts.

2.2. Bounce Rock

Bounce Rock is a 40 cm exotic rock that was discovered by the Opportunity rover in the bounce mark of the lander's airbag. The dark, fine-grained rock is unlike any other rock examined by Opportunity and was likely delivered to the site as secondary impact ejecta (Joliff et al., 2006). Three areas of Bounce Rock were examined by APXS, including two "as is" rock surfaces (Glanz and Maggie) and one RAT ground spot (Case). The RATted Case is lower in SO_3 (0.56 vs. 3.66 and 4.63 wt%) and higher in SiO_2 (51.6 vs. 48.5 and 47.5 wt%) than the "as is" surfaces. The Mössbauer examined 7 different spots on this rock. Compositionally Bounce Rock is like the basaltic shergottites EET A79001 (lithology B) and Zagami (Rieder et al., 2004; Zipfel et al., 2011).

3. Mössbauer and measured Fe^{3+}/Fe_{Total}

The MIMOS II Mössbauer spectrometer onboard the Mars Exploration Rovers (Klingelhöfer et al., 2003) provides *in situ* quantitative information about the distribution of Fe among its oxidation and coordination states, allowing for the identification of Fe-bearing mineral phases. The relative distribution of Fe between those phases is found by analysis of Mössbauer subspectral areas (A). In order to estimate proportions of Fe-bearing minerals, assumptions of mineral chemistry must be made (e.g., Morris et al., 2004; McSween et al., 2008). The methodology for Mössbauer spectral analysis is provided by Morris et al. (2006a, 2006b, 2008).

The partitioning of iron between Fe-bearing mineral phases in the Gusev basalts is determined by the positions of sextet or doublet peaks relative to reference sample Mössbauer spectra (Table 1; Morris et al., 2006a, 2006b; 2008). Olivine, pyroxene, and magnetite were identified in all Gusev basalts, although their relative proportions vary; olivine/pyroxene ratios range from 1.42 to 0.09 for the Adirondack and Irvine classes, respectively. Mössbauer spectral analysis of the magnetite sextet peaks yields the distribution of Fe between octahedral and tetrahedral sites in magnetite; Morris et al. (2008) assumes Fe^{3+} is housed in the Fe3S1 tetrahedral and half of the Fe2.5S1 octahedral sites to find bulk rock Fe^{3+}/Fe_T). In ideal stoichiometric magnetite, the ratio of octahedral to tetrahedral Fe is 2. Substitution of major and minor elements Mg, Al, Ti, Mn, and Cr, and trace elements Ni, Zn, and V likely accounts for the nonstoichiometric distribution of Fe observed for the Gusev basalts (Fe2.5S1/Fe3S1 = 0.8 to 1.6). Solid solutions on phases containing these elements (e.g., ulvöspinel; Fe_2TiO_4) with magnetite cannot be distinguished at low concentrations. In particular, titanomagnetite is consistent with variations in Fe and Ti in APXS spectral areas of dust captured by magnets on the Spirit and Opportunity rovers (Madsen et al., 2009) and with oxide mineral compositions of basaltic shergottites, which range from titanomagnetite to nearly pure ulvöspinel (McSween and Treiman, 1998). Ilmenite was identified in only minor amounts in Backstay (3% of the subspectral area). The only igneous Fe-bearing mineral found in Bounce Rock is pyroxene (95 to 99%; Morris et al., 2006b; Zipfel et al., 2011).

Surface alteration and/or devitrification are indicated by secondary ferric oxides (hematite and nanophase ferric oxide, npOx) comprising a portion of Mössbauer spectral areas. Among the more massive basalts, npOx makes up 1 to 13% of the spectral areas (Table 1; Morris et al., 2006a). The clastic Barnhill class has experienced more pervasive alteration as evidenced by npOx composing up to 30% of the spectral area. The npOx is interpreted to be a product of local low temperature alteration (Morris et al., 2006a) and may reflect oxidation and devitrification of volcanic glass (Schmidt et al., 2009).

Fe^{3+}/Fe_T for Gusev basalt rock surfaces indicated by Mössbauer (Table 1) range from 0.17 for the rock interiors of the comparatively unaltered Adirondack class to 0.36–0.4 for the unbrushed surfaces of Irvine class basalts to 0.51–0.53 for the more altered Barnhill class. These values are too high to be primary and include contributions by secondary ferric oxides. Even so, the measured Fe^{3+}/Fe_T values represent uppermost estimates for magmatic fO_2 conditions (Method 1; Table 2). We calculate fO_2 relative to QFM using Eq. (7) of Kress and Carmichael (1991; see Table 2 caption) and assuming reasonable magmatic temperature (1500 K) and current Mars atmospheric pressure (1150 Pa). The estimated fO_2 for the Adirondack and Backstay classes are more reduced than the QFM buffer. The more altered Barnhill class rocks range from 2.7 to 3.0 log units above QFM.

Apart from 0–3% surface dust ascribed to npOx, Bounce Rock is monomineralic (pyroxene only) with respect to iron. The Fe^{3+}/Fe_T

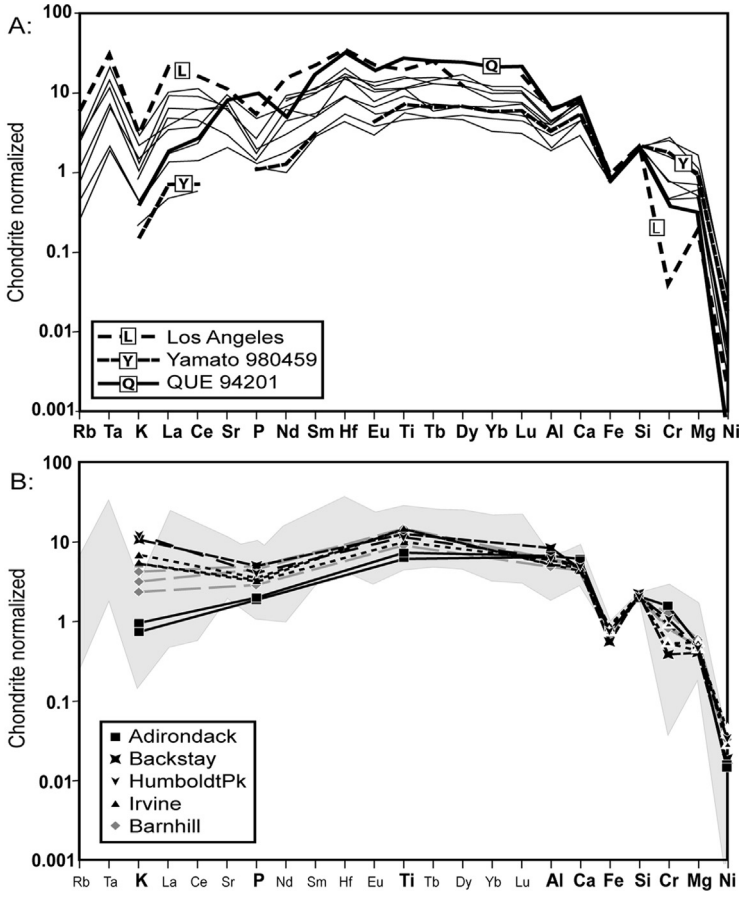

Fig. 2. Chondrite normalized element abundance diagrams for (A) basaltic and olivine-phyric shergottites and (B) Gusev basalts. The gray region in B corresponds to the range in shergottites in A. C1 chondrite element abundances are from Sun and McDonough (1989). Figure is modified after Schmidt and McCoy (2010).

Table 1
Percent Mössbauer spectral areas and measured Fe^{3+}/Fe_T (Morris et al., 2008).

Generic name assignment target	Type[1]	Class	Fe2D1 Ol	Fe2D2 Px	Fe2D3 Ilm	Fe3D1 NpOx	Mt	Fe3S1 Mt(tet)	Fe2.5S2 Mt(oct)	Fe3S2 Hm	Ol/Mt	Fe^{3+}/Fe_T
Gusev Crater[2]												
Adirondack	RR	*Adirondack*	47	33	0	6	13	5	8	1	3.62	0.17
Humphrey	RR	*Adirondack*	47	34	0	7	11	6	5	2	4.27	0.17
Backstay	RB	*Backstay*	35	37	3	13	11	5	6	2	3.18	0.20
Irvine	RU	*Irvine*	10	45	0	6	35	17	19	3	0.29	0.36
Esperanza	RU	*Irvine*	4	46	0	4	46	25	20	1	0.09	0.4
Barnhill_Ace	RU	*Barnhill*	18	22	0	29	26	11	15	5	0.69	0.53
Posey	RB	*Barnhill*	17	23	0	26	32	16	16	3	0.53	0.53
CoolPapaBell	RB	*Barnhill*	17	24	0	30	27	12	12	3	0.62	0.51
Humboldt Pk	RU	*Humboldt Pk*	53	10	0	11	29[4]	(14)	(15)	0	1.83	0.31
Meridiani Planum[3]												
Bounce Rock_Glanz2	RU	*Bounce Rock*	0	98	0	3	0	0	0	0	0	0.03
Bounce Rock_Case	RR	*Bounce Rock*	0	99	0	1	0	0	0	0	0	0.01
Bounce Rock_Maggie	RU	*Bounce Rock*	0	95	0	5	0	0	0	0	0	0.05

Uncertainties are ±2% absolute (Morris et al. 2006a, 2006b, 2008).
[1] RR is RAT-abraded rock; RB is RAT-brushed rock; and RU is as is rock surface.
[2] Morris et al. (2008).
[3] Zipfel et al. (2011).
[4] Assumes Mt(oct) : Mt(tet) ratio of 1.1 because crystallographic site assignments are not reported by Morris et al. (2008), and this value is consistent with other Gusev basalts.

of the Bounce Rock targets are consequently very low (0.01 to 0.05), where all Fe^{3+} is from secondary npOx (Zipfel et al., 2011). The calculated fO_2 values are also low (−4.05 to −7.81 ΔQFM), or less than or equal to the iron-wüstite buffer (as defined by Holloway et al., 1992). Metallic iron was not identified in Bounce Rock, suggesting that these fO_2 estimates are too low to be realistic (e.g., McCanta et al., 2004).

4. Methods to estimate primary magmatic fO_2

We here present three other methods to estimate magmatic fO_2 conditions by removing secondary npOx and hematite. The first two methods make use of the distribution of Fe between igneous mineral phases as determined by Mössbauer spectral analysis. The third incorporates elemental compositions by finding Fe^{3+}/Fe_T as

Table 2
Estimated Fe^{3+}/Fe_T and ΔQFM for Basaltic rocks in Gusev Crater.

Target	Class	*Method 1: Measured*		*Method 2a: Igneous Mins*		*Method 2b: Mt substitution*		*Method 3: Normative Fa/Mt*	
		Fe^{3+}/Fe_T	ΔQFM*	Fe^{3+}/Fe_T	ΔQFM*	Fe^{3+}/Fe_T	ΔQFM*	Fe^{3+}/Fe_T	ΔQFM*
Adirondack	*Adirondack*	0.17	−0.7	0.10	−2.2	0.09	−2.4	0.10	−2.1
Humphrey	*Adirondack*	0.17	−0.8	0.09	−2.3	0.05	−3.6	0.08	−2.6
Backstay	*Backstay*	0.23	−0.2	0.09	−2.6	0.07	−3.3	0.12	−2.0
Irvine	*Irvine*	0.36	1.5	0.29	0.8	0.21	−0.2	0.26	0.4
Esperanza	*Irvine*	0.4	1.9	0.36	1.5	0.21	−0.2	0.28	0.7
Barnhill_Ace	*Barnhill*	0.53	3.0	0.28	0.6	0.23	0.0	0.25	0.2
Posey	*Barnhill*	0.53	2.8	0.33	1.0	0.22	−0.2	0.29	0.6
CoolPapaBell	*Barnhill*	0.51	2.7	0.26	0.4	0.18	−0.8	0.22	−0.2
Humboldt Pk	*Humboldt Pk*	0.31	0.7	0.23	−0.1	0.16	−1.2	0.21	−0.4
Bounce Rock_Glanz2	*Bounce Rock*	0.03	−5.3	–	–	–	–	–	–
Bounce Rock_Case	*Bounce Rock*	0.01	−7.8	–	–	–	–	–	–
Bounce Rock_Maggie	*Bounce Rock*	0.05	−4.1	–	–	–	–	–	–

*Calculated relative to the quartz–fayalite–magnetite (QFM) buffer (Wones and Gilbert, 1969) and solved using Eq. (7) of Kress and Carmichael (1991) at $T = 1500$ K and current Mars atmospheric pressure ($P = 1150$ Pa), where

$$\ln\frac{X_{Fe_2O_3}}{X_{FeO}} = a\ln(f_{O_2}) + \frac{b}{T} + c + \sum_i d_i X_i + e\left[1 - \frac{T}{T_o} - \ln\left(\frac{T}{T_o}\right)\right] + f\frac{P}{T} + g\frac{(T-T_o)P}{T} + h\frac{P^2}{T}.$$

X_i is the mole fraction of element i. We assume that $T = T_o$. Parameter values for this equation are $a = 0.196$; $b = 1.1492 \times 10^4$ K; $c = -6.675$; $d_{Al_2O_3} = -2.243$; $d_{FeO_*} = -1.828$; $d_{CaO} = 3.201$; $d_{Na_2O} = 5.854$; $d_{K_2O} = 6.215$; $e = -3.36$; $f = -7.01 \times 10^{-7}$ KPa^{-1}; $g = -1.54 \times 10^{-10}$ Pa^{-1}; $h = 3.385 \times 10^{-17}$ KPa^{-2}.

a function of a CIPW normative mineral ratio (fayalite/magnetite). These methods were not applied to Bounce Rock because it does not contain any magnetite and is quartz normative (Zipfel et al., 2011).

4.1. fO_2 by igneous minerals

As a relatively straightforward method to estimate magmatic fO_2, (Method 2a) we first calculate the ratio Fe^{3+}/Fe_T of the Fe-bearing igneous minerals determined by Mössbauer spectral analysis (Table 1; Morris et al., 2006a, 2006b, 2008) according to

$$\left(Fe^{3+}/Fe_T\right)_{ignmins} = \frac{(Mt(tet) + 0.5Mt(oct))}{(Ol + Px + Ilm + Mt)}. \quad (1)$$

For this calculation, we assume that Fe in olivine and pyroxene is entirely in the 2+ valence state, although up to 7.9% and 2.3% Fe^{3+} have been identified in shocked olivine and pyroxene separates, respectively, of the shergottitic meteorites (Dyar, 2003). This method also assumes that all magnetite is primary (i.e., not the result of serpentinization of olivine or other hydrothermal processes; e.g., Ehlmann et al., 2010; Schmidt et al., 2009) and does not account for magnetite solid solution.

To better account for the nonstoichiometric distribution of Fe between the octahedral and tetrahedral crystallographic sites in magnetite and likely solid solution with Ti, Al, and Cr-bearing spinel endmembers, we also present a second method to find Fe^{3+}/Fe_T of the igneous mineral assemblage (Method 2b: Mt substitution; Table 2). The substitution of trivalent or tetravalent cations in magnetite is most commonly balanced by ferrous iron in the form of hercynite ($Fe^{2+}Al_2O_4$), chromite ($Fe^{2+}Cr_2O_4$), or ulvöspinel ($Fe_2^{2+}TiO_4$). For Method 2b, Fe is allocated between the different valence states in magnetite (Mössbauer subspectral areas of Fe3S1 and Fe2.5S1) by first determining how much Fe fits into ideal magnetite (Mt*) with an octahedral/tetrahedral ratio of 2 and then stoichiometrically assigning Fe between the valence states; the remaining Fe is assumed a 2+ valence (Table 3). The Fe^{3+}/Fe_T of the magnetite phase by this method varies from 0.43 to 0.62. Substitution of divalent cations for octahedral Fe^{2+} is not taken into account by this calculation, but is likely minor because compositions of magnetites and ulvöspinels in the shergottite and nakhlite meteorites typically contain <1 wt% of each MgO and MnO (e.g., McSween and Treiman, 1998). The Fe^{3+}/Fe_T of the igneous assemblage is then found as the ratio of Fe^{3+} in magnetite to the total Fe in the igneous assemblage (Ol, Px, Ilm, Mt).

Table 3
Distribution of Fe between ideal and nonideal magnetite for Method 2b.

Target	Mt[1]	Mt*[2]	Mt–Mt*[3]	Fe^{3+}/Fe_T in Mt
Adirondack	13	12	1	0.62
Humphrey	11	7.5	3.5	0.45
Backstay	11	9	2	0.55
Irvine	35	28.5	6.5	0.54
Esperanza	46	30	16	0.43
Barnhill_Ace	26	22.5	3.5	0.58
Posey	32	24	8	0.50
CoolPapaBell	27	18	9	0.44
Humboldt Pk	29	22.5	6.5	0.52
Ideal magnetite (Mt*)				*0.67*

[1] Mt is the % subspectral area of Fe3S1 + Fe2.5S2 (Table 1).
[2] Mt* is ideal stoichiometric magnetite ($Fe^{3+}(Fe^{2+}Fe^{3+})O_4$) and includes all Mt(oct) and corresponding Mt(tet) at a 2:1 ratio (Table 1).
[3] Mt–Mt* is the remaining Fe and is assigned a 2+ valence.

Estimates of magmatic fO_2 that account for magnetite solid solution (Method 2b) range from −3.6 to 0.0 ΔQFM and are in all cases lower than estimates based igneous mineral that do not (Method 2a; −2.6 to +1.5 ΔQFM). The Adirondack and Backstay classes contain the least magnetite and as a consequence have the lowest estimated fO_2 by both igneous minerals methods (−2.6 to −2.2 ΔQFM by 2a; −3.6 to −2.4 ΔQFM by 2b). Other basalt classes, including the more altered Barnhill, are more oxidized and yield roughly similar estimates between them depending on the method used (−0.1 to +1.5 ΔQFM by 2a; −1.2 to 0.0 ΔQFM by 2b).

4.2. Influence of Fe^{3+}/Fe_T on CIPW norm

APXS geochemical data (Gellert et al., 2006; Ming et al., 2008) can be recast into normative minerals using the standard CIPW norm calculation procedure (e.g., McSween et al., 2004). The CIPW norm assumes 100% equilibrium crystallization at 1 atm and is strongly dependent on the input Fe^{3+}/Fe_T. As Fe^{3+}/Fe_T increases, normative magnetite increases, which increases the degree of silica saturation, causing normative olivine to decrease until quartz is normative (Fig. 3). The CIPW norm calculation assumes pure endmember phases and does not account for solid solution in magnetite. Other workers have used Fe^{3+}/Fe_T determined by Mössbauer to find the CIPW normative mineralogy, but there are

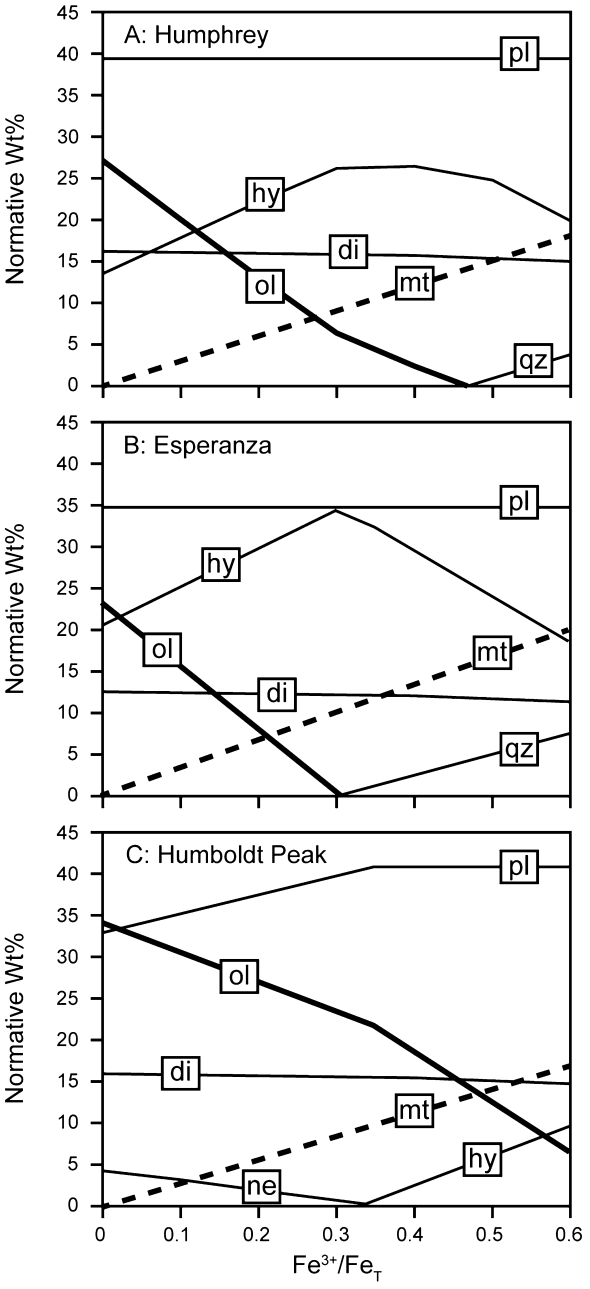

Fig. 3. CIPW normative mineral abundances as a function of Fe^{3+}/Fe_T for representative Gusev basalts. (A) Adirondack class Humphrey; (B) Irvine class Esperanza; and (C) Humboldt Peak (pl = plagioclase, di = diopside, hy = hypersthene, ol = olivine, mt = magnetite, qz = quartz, ne = nepheline).

important inconsistencies including higher measured olivine content than expected by the norm calculations (e.g., McSween et al., 2004, 2006a, 2006b).

To infer magmatic fO_2, we iteratively determined the Fe^{3+}/Fe_T until the CIPW normative mineralogy matched mineral contents determined by Mössbauer. More specifically, we found at what Fe^{3+}/Fe_T the ratio of normative fayalite/magnetite (Fa/mt) matches the olivine/magnetite (ol/mt) found by Mössbauer. The Fa/mt parameter was used because these minerals are sensitive to Fe^{3+}/Fe_T (Fig. 3) and are found in all Gusev basalts (Table 1). In doing so, we assume that measured olivine/magnetite ratios reflect the igneous assemblage and there has been no later alteration such as olivine dissolution (e.g., Tosca et al., 2004) or magnetite mineralization (e.g., Schmidt et al., 2009).

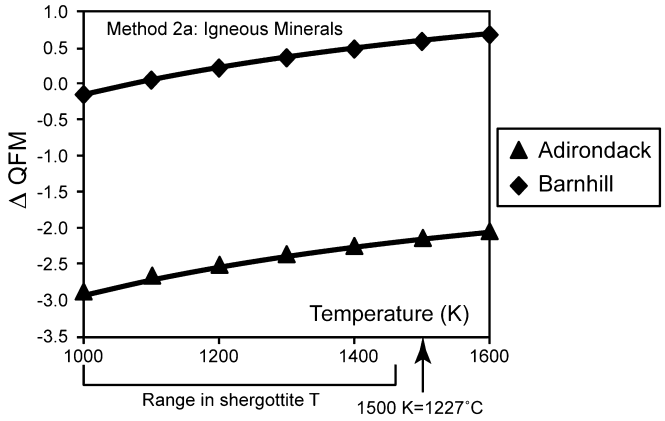

Fig. 4. Calculated ΔQFM based on Fe^{3+}/Fe_T determined by igneous minerals as a function of temperature (by Eq. (7) of Kress and Carmichael, 1991; Table 2 caption). For our calculations, we assume near liquidus temperatures of 1500 K. The range in shergottite temperatures is from fO_2 estimates by Goodrich et al. (2003), Herd et al. (2001), and Herd (2003).

The Fe^{3+}/Fe_T and fO_2 estimated by normative mineralogy generally fall between those estimates based on the igneous mineral assemblages determined by Mössbauer spectroscopy (Table 2). The one exception is Backstay, which is the only basalt with detectable ilmenite (3%; Table 1). Estimates for fO_2 by Method 3 vary from −2.6 ΔQFM for the Adirondack class rock Humphrey to +0.7 ΔQFM for the rock Esperanza of the Irvine class.

5. Discussion

5.1. How to interpret estimates of fO_2

In all cases, measured bulk rock Fe^{3+}/Fe_T of the Gusev basalts by Mössbauer spectrometer yield higher Fe^{3+}/Fe_T (0.17 to 0.53) than by other methods (0.05 to 0.36). This is because all targets contain at least some secondary ferric phases, such as nanophase Fe-oxides or hematite, for which the other methods correct. In this section, we discuss confidence levels and geologic processes that may affect estimates for igneous fO_2.

One source of concern for relating our Gusev estimates to those for the martian meteorite samples is the observation that Fe^{3+}/Fe_T found in SNC meteorites by Mössbauer spectroscopy and XANES do not correlate with fO_2 by other methods. The interpreted cause of this observation is dehydrogenation or hydrogen loss during shock metamorphism (Dyar, 2003). The Gusev basalts do not exhibit textural evidence for shock and while it is impossible to rule out, we assume igneous and weathering processes are more likely to affect the Fe^{3+}/Fe_T in these rocks. The lack of correlation between fO_2 and Fe^{3+}/Fe_T in the SNCs emphasizes the importance of converting Fe^{3+}/Fe_T to fO_2 in order to compare the martian dataset.

The calculation of fO_2 relative to the QFM buffer from Fe^{3+}/Fe_T invites its own set of assumptions, which include temperature and pressure conditions. Fig. 4 illustrates the dependence of ΔQFM as a function of temperature for Adirondack and Barnhill by Method 2a (igneous minerals). The estimates presented in Table 2 assumed the temperature is near the liquidus at 1500 K (1227 °C) for all Gusev basalts. Oxybarometry of the shergottitic meteorites indicates a larger range of temperatures that extend to lower values (1003–1459 K; Herd et al., 2002; Herd, 2003) than we assume for the Gusev basalts. The meteorites are more coarse-grained and fully crystallized however, suggesting that their mineral assemblages reflect more subsolidus re-equilibration and lower temperatures than the crystal-poor to aphyric Gusev basalts. More importantly, the temperature dependence of fO_2 relative to QFM (Fig. 4) suggests that relative differences between estimates are more real

than the calculated ΔQFM values. Temperature dependence alone suggests uncertainties on our estimates are at least ±0.5 log units ΔQFM.

Alteration of basaltic rocks at the martian surface also affects proportions of igneous minerals. Under the oxidizing, acidic conditions of the modern martian environment, olivine dissolves more rapidly than pyroxene and magnetite (e.g., Hausrath et al., 2008). Lower olivine/magnetite ratios and MgO concentrations observed in weathering rinds than in RAT-abraded interiors of the Adirondack basalts are consistent with ~20% dissolution of Fo50 olivine (Hurowitz et al., 2006). Olivine dissolution at rock surfaces can thus lead to higher Fe^{3+}/Fe_T found by all 3 methods. To test its influence on these estimates, we added 20% olivine to brushed and unbrushed surface analyses and found a decrease in calculated Fe^{3+}/Fe_T by ~5%, with a difference of −0.03 to −0.22 ΔQFM. While uncertainties of this calculation make it not worth pursuing further, the effects of low temperature alteration at the martian surface is an important caveat to bear in mind.

In addition, serpentinization and/or hydrothermal alteration may generate secondary magnetite at the expense of olivine (e.g., Ehlmann et al., 2010) and would increase calculated Fe^{3+}/Fe_T. There is no evidence for secondary magnetite in the Adirondack, Irvine, Backstay, and Humboldt Peak classes. The Pesapallo subclass of Barnhill found along the east side of Home Plate however, has a greater proportion of magnetite (42–54% of the Mössbauer subspectral area) and less olivine (1–2%) than other Barnhill class rocks (24–28% magnetite and 17–18% olivine; Morris et al., 2008). The difference in mineral contents with little change in elemental composition (higher Zn and Ni in Pesapallo) across Home Plate is interpreted to reflect hydrothermal alteration that has affected the Pesapallo rocks (Schmidt et al., 2009). For this reason, the Pesapallo subclass was left out of our calculations.

Because Method 2a assumes that all the tetrahedral and 50% of the octahedral sites in magnetite contain Fe^{3+}, we consider these estimates to be too high. This assumption is not consistent with nonstoichiometric distribution of Fe between the sites determined by Mössbauer spectroscopy (Mt(oct)/Mt(tet) < 2). In addition, almost none of the shergottitic meteorites contain pure magnetite and instead contain titanomagnetite to nearly pure ulvöspinel, Fe-rich spinel, or chromite (e.g., McSween and Treiman, 1998). The one exception is the magnetite-bearing basaltic breccia NWA 7034 and its high estimated fO_2 (+1 to +3 ΔQFM) is interpreted to reflect post-magmatic conditions (Agee et al., 2013b).

The primary fO_2 for the Gusev basalts likely lies somewhere between our estimates by Methods 2b (igneous minerals accounting for magnetite substitution) and 3 (normative Fa/Mt) with a degree of uncertainty. An iron-rich basaltic magma at first fractionally crystallizes minerals that are less oxidized than the melt, driving the melt composition to higher fO_2 (as much as 1 log unit ΔQFM), until Fe–Ti oxide saturation when fO_2 and FeO* concentration begin to decrease (Toplis and Carroll, 1996). All Gusev basalts have 11–46% of their Mössbauer spectral areas assigned to magnetite (Table 1) and so interpretation of the fO_2 estimates depends on how far the magmas are along a liquid line of descent. High MgO (up to 10.8 wt%) and a general correlation between FeO* and SiO_2 for the Adirondack, Irvine, and Humboldt Peak basalt groups (Fig. 1B), suggests relative primitiveness of these rocks and that little (titano)magnetite has been removed. Assuming in-place fractional crystallization of basaltic lavas, the fO_2 estimated by Method 2b captures the early part of crystallization and represents a minimum estimate, while the fO_2 by normative Fa/mt assumes 100% crystallization and represents a maximum estimate.

High SiO_2, low FeO* as well as relatively low magnetite contents found in the Backstay target may suggest that in contrast to the other Gusev basalt groups, the Backstay magma underwent magnetite (or magnetite solid solution series) fractionation during its petrogenesis (Fig. 1B; Table 1). This interpretation is consistent with models by McSween et al. (2006a, 2006b) that generate Backstay compositions by fractionation of a Humphrey-like parent and include Fe-oxide (early chromite to late ulvöspinel/magnetite) throughout the crystallization sequence. The evolved nature of Backstay may then suggest that the estimated ΔQFM is 1–2 log units lower than its parental magma (i.e., decoupled from its mantle source). Alternatively, the Backstay magma may have formed by low degree partial melting of the mantle (Schmidt and McCoy, 2010) and our fO_2 estimates would therefore reflect its mantle source.

The ranges of fO_2 estimated by Methods 2b and 3 (−3.6 to +0.7 ΔQFM) represent our best estimates for primary igneous fO_2 for the Gusev basalts. The observation that metallic iron is not identified in the Gusev basalts provides an independent calibration for our estimates and indicates that the absolute minimum fO_2 is not significantly below the iron-wüstite (IW) buffer (e.g., McCanta et al., 2004 found exsolved metallic Fe in 1-atm experiments on Mars-relevant compositions equilibrated at fO_2 = IW and IW-1). Relative differences between our estimates are more robust than the values we present, and one should be mindful of the effect of alteration processes. With these caveats in mind, our level of confidence is ±0.5 to 1 log units ΔQFM, which is not much worse than errors presented for lab-based measurements of fO_2 in martian meteorites (e.g., ±0.5 log QFM; Wood, 1991).

5.2. Comparison with other planetary basalts

A compilation of fO_2 values for Mars, Earth and the Moon is presented in Fig. 5. In spite of the uncertainties to our methods, it is striking how the overall range in fO_2 that we estimate for the Gusev basalts (−3.6 to +0.7 ΔQFM) is very similar to what has been estimated for magmatic conditions of the shergottitic meteorites (−3.7 to +0.3 ΔQFM; Goodrich et al., 2003; Herd et al., 2001, 2002; Herd, 2003, 2006; Peslier et al., 2010; Szymanski et al., 2010). Higher values of fO_2 have been estimated for the nakhlites (up to +1.5 ΔQFM for MIL 03346; Dyar et al., 2005) and for post-magmatic conditions of the basaltic breccia NWA 7034 (+1 to +3 ΔQFM; Agee et al., 2013b). The striking similarity between the ranges for magmatic fO_2 for the martian basalts from both landed and meteorite datasets however, indicates that the fO_2 of the source mantle is relatively restricted and we have yet to identify an exotic mantle reservoir with respect to fO_2.

Our direct estimates for fO_2 of the relatively unaltered Gusev basalts are in contrast to recent models by Tuff et al. (2013) that suggest more oxidized conditions (+2 to +3 ΔQFM) during mantle partial melting and subsequent igneous differentiation to generate the entire Gusev suite, including soils, and unbrushed and hydrothermally altered rocks and to account for compositional differences between the Gusev and SNC datasets. Our estimates do not range to the oxidized values common to terrestrial arc magmas, but they are also not quite as reduced as lunar Mare basalts (Frost and McCammon, 2008; Sato et al., 1973; Sato, 1978).

The Gusev basalts seemingly fall into two groups of contrasting fO_2 conditions, where more reduced values (−2.7 ΔQFM average) are found for the Adirondack and Backstay classes and more oxidized values (−0.1 ΔQFM average) are found for the Humboldt Peak, Irvine, and Barnhill classes. Our estimates of primary fO_2 for the olivine-rich Adirondack and Backstay classes are comparable to ranges for the most reduced olivine-phyric shergottites (SaU 005, Dhofar 019, Y980459, and NWA 57089; Herd, 2003, 2004; Gross et al., 2011). High-Mg Adirondack class basalts and the olivine-phyric shergottites are therefore likely partial melts of similarly reduced mantle. Backstay basalt may likewise be a partial melt of reduced mantle, but it is also more evolved (higher SiO_2) and may

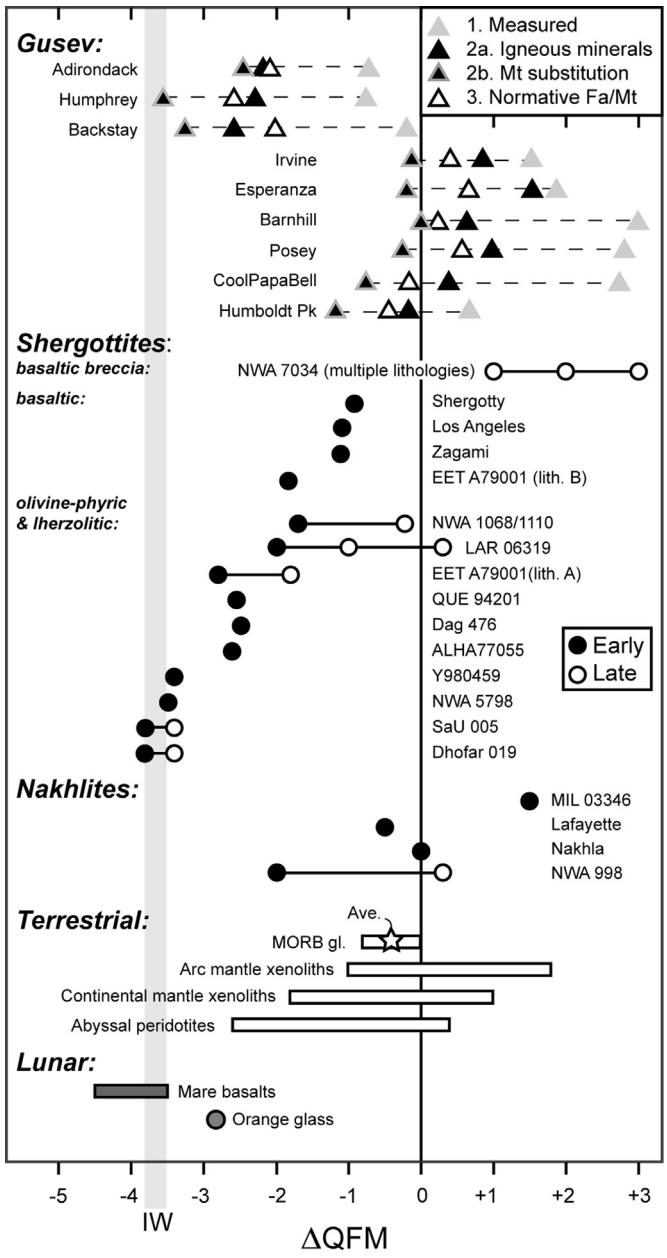

Fig. 5. Compilation of fO_2 of Mars, Earth, and the Moon relative to QFM (as defined by Wones and Gilbert, 1969). The position of the iron-wüstite buffer (IW as defined by Holloway et al., 1992) depends on temperature and is approximated by the gray field. Early and late fO_2 estimates for individual meteorites are based on petrographic interpretations by Goodrich et al. (2003) and Herd (2006). Data are from this study, Agee et al. (2013b), Dyar et al. (2005), Frost and McCammon (2008), Goodrich et al. (2003), Gross et al. (2011), Herd et al. (2001, 2002), Herd (2003, 2004), Peslier et al. (2010), Sato et al. (1973), Sato (1978), and Szymanski et al. (2010). Note that estimates for NWA 7034 are from 3 different lithologies and estimates are interpreted to record post-magmatic fO_2 (Agee et al., 2013b).

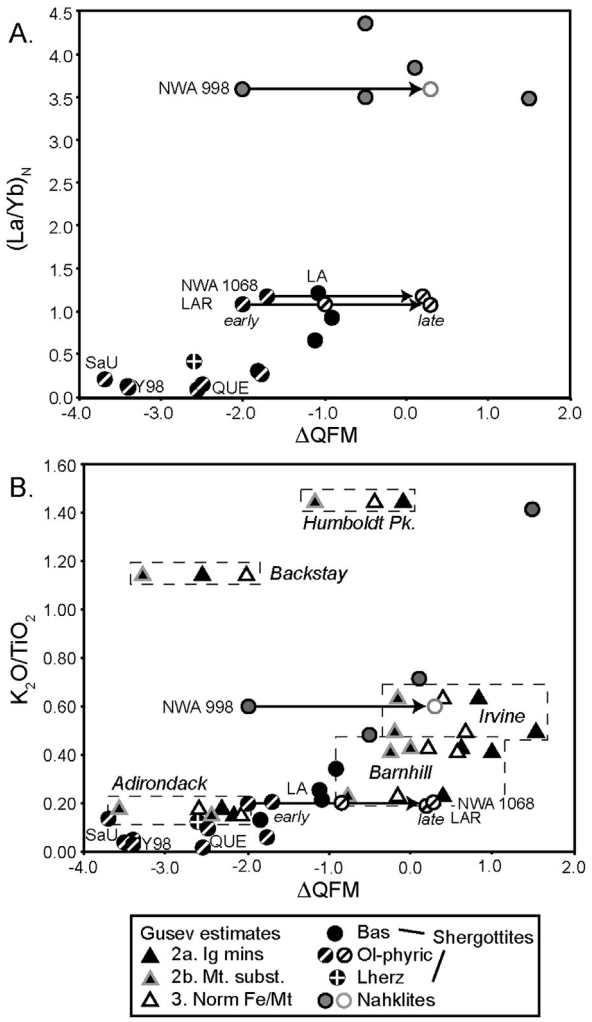

Fig. 6. Plots of indices for incompatible element enrichment in the shergottitic and nahklite meteorites and Gusev basalt versus estimates for ΔQFM. A) Chondrite normalized LREE enrichment $(La/Yb)_N$ correlates with estimates of fO_2 in the shergottitic meteorites (Herd et al., 2002). Selected meteorites are indicated (NWA 1068 is paired with NWA 110; LAR is LAR 06319; SaU is SaU 005; Y98 is Y980459; and QUE is QUE 94201.) B) A proxy for LREE enrichment among the Gusev basalts is K_2O/TiO_2, and it also correlates with ΔQFM for the martian basalts, excepting the Gusev basalt Backstay. (Note difference in scale.) This relation suggests involvement of melts or fluids from at least two reservoirs with contrasting fO_2 and agrees with models proposed for the SNC meteorites (e.g., Herd, 2003, 2006). Data are from Goodrich et al. (2003), Herd et al. (2001, 2002), Herd (2003, 2006), Meyer (2013), Peslier et al. (2010), Schmidt and McCoy (2010), and Szymanski et al. (2010).

have instead undergone magnetite series fractionation. Estimates for Backstay magmatic fO_2 therefore may or may not be decoupled from its mantle source.

The higher range of fO_2 estimated for the Irvine, Humboldt Peak, and Barnhill classes (−1.2 to +0.7 ΔQFM) are more similar to the more evolved basaltic shergottites (Shergotty, Zagami, and Los Angeles), and the nakhlites Lafayette and Nakhla. In addition, the more oxidized Gusev basalts are like the higher fO_2 estimates for the late mineral assemblages of olivine-phyric basaltic shergottites NWA 1068/1110 and LAR 06319 and nakhlite NWA 998 reflecting changes during fractional crystallization (Fig. 5; Goodrich et al., 2003; Herd et al., 2001, 2002; Herd, 2003, 2006; Peslier et al., 2010; Szymanski et al., 2010). These similarities suggest involvement of a more oxidized reservoir during the petrogenesis of these magmas.

5.3. Correlation with tracers for reservoirs in the martian interior

Among the shergottitic meteorites, Herd et al. (2002) noted a correlation between fO_2 and La/Yb (Fig. 6A) and initial $^{87}Sr/^{86}Sr$ calculated at 175 Ma and suggested this correlation reflects mixing between melts derived from at least two reservoirs with contrasting fO_2. Such contrasting reservoirs may represent reduced, light rare earth element (LREE)-depleted mantle and more oxidized, LREE-enriched crust (Herd et al., 2002), or two distinct mantle sources formed during the differentiation of the magma ocean (e.g., Herd, 2003). The LREE-enriched, high fO2 nature of the nakhlites also supports the existence of an oxidized reservoir in the martian interior. A recent study by McCubbin et al. (2013) suggests

that the oxidized nature of the nakhlites may have formed by degassing of a Cl-rich fluid which preferentially partitioned Fe^{2+} into the fluid phase (McCubbin et al., 2013). Differences in Nd and W isotopic ratios suggest the nakhlite source is distinct from the contaminant for the enriched basaltic shergottites and metasomatised. An alternative model suggests that the nakhlite melt–melt depleted residue may have combined with another deep mantle reservoir to generate the depleted shergottites (Blinova and Herd, 2009).

Although there are no REE or isotopic data for the Gusev basalts, there is a correlation between the estimated fO_2 of four Gusev basalt classes (Adirondack, Barnhill, Irvine, and Humboldt Peak) and enrichments in incompatible trace elements (K_2O/TiO_2; Fig. 6B). Variations in K_2O/TiO_2 versus fO_2 for the Gusev basalts generally overlap with those of the SNC meteorites (excepting Backstay and early NWA 998). Additionally, these variations suggest two-component mixing between melts derived from a reduced, K and LREE-poor reservoir and from a more oxidized LREE-rich reservoir, such as has been suggested for the basaltic and olivine-phyric shergottites (Herd et al., 2002). Of the martian basalts, Adirondack class and olivine-phyric shergottites (e.g., Yamato 980459) are the most likely direct mantle melts (e.g., Herd, 2004; Monders et al., 2007; Borg and Draper, 2003) and are representative of a reduced, LREE-depleted reservoir. The alkali-rich Irvine and Humboldt Peak basalts as well as the more evolved basaltic shergottites have likely interacted with an LREE-rich, oxidized reservoir.

5.4. fO_2 and implications for the evolution of Mars

The limited range in estimated fO_2 for martian basalts and the martian interior is significant for our understanding of Mars evolution. The exterior of Mars is very oxidized, as indicated by the high Fe^{3+}/Fe_T that have been measured in weathered and/or hydrothermally altered materials by the Mössbauer spectrometer (up to 0.93 in Montalva in Gusev Crater; Morris et al., 2008). In contrast, our maximum estimated igneous Fe^{3+}/Fe_T is 0.29. This indicates that tectonic processes have not led to sufficient recycling of oxidized surface material into the interior to entirely affect the overall oxidation state of the martian mantle.

There also appears be a limit to how much fO_2 may increase in the Mars interior by normal mantle processes. Magma mixing, such as has been interpreted for the generation of the observed variability in fO_2 between the depleted and enriched shergottites (Herd et al., 2002), is limited by the endmember fO_2. However, the existence of at least two reservoirs with co-varying LREE-enrichment and oxygen fugacity points towards some mechanism to adjust these compositional parameters that is possibly related to planetary differentiation. Sm–Nd systematics in olivine-phyric shergottites support early formation of the depleted mantle reservoir by 4.525 Ga (Borg et al., 1997). The more oxidized, LREE-rich reservoir may signify involvement of the crust or mantle source heterogeneities formed during early differentiation of the planet.

Our estimates of fO_2 for the Gusev basalts also support the existence of at least two reservoirs with distinct incompatible element and fO_2 characteristics by the Early Hesperian. Differences in composition among the Gusev basalts have been suggested to arise by fractional crystallization (McSween et al., 2006b), but magnetite series fractionation limits the degree to which fO_2 may increase by this process alone (Toplis and Carroll, 1996). The observed trace element variations may also be generated by varying degrees of partial melting, or by multi-stage batch partial melting of WD model mantle (Wänke and Dreibus, 1988), although some additional K (0.01 wt% vs. 0.003 wt% in WD mantle) is necessary to produce the observed K concentrations at melt fractions sufficient to allow melt migration (Schmidt and McCoy, 2010). At degrees of partial melting not sufficient to entirely change the residual mineralogy of WD mantle, the fO_2 of the melt would retain the fO_2 of its mantle source. One possible mechanism to introduce both additional K and more oxidizing conditions is by metasomatism, involving a reaction of aqueous fluids with the martian mantle (e.g., Borg and Draper, 2003; Treiman, 2003). Such a process would generate an inhomogeneous distribution of K in the martian mantle, which is necessary to (a) explain differences in alkalis observed between the Gusev basalts and SNC meteorites, and (b) generate realistic crustal thicknesses in thermal and chemical evolution models (e.g., Hauck and Phillips, 2002; Ruedas et al., 2013). Alternatively, assimilation of the crust may enrich Gusev primary melts in K_2O/TiO_2 and increase magmatic fO_2.

Because we are working with a limited dataset, we will likely continue to revise conceptual models regarding the evolution of oxygen fugacity and incompatible element compositions in the martian mantle, particularly were isotopic data to become available, either by in situ measurement or returned samples. There is also a possibility that more oxidized basaltic igneous rocks exist. The relationship of increasing K_2O/TiO_2 with fO_2 may extend, for example, to the recently discovered mugearite Jake_Matijevic in Gale Crater by the Curiosity rover ($K_2O/TiO_2 = 2.6–4.4$); petrochemical modeling suggests its evolved alkaline composition may have formed by plagioclase-free fractional crystallization of a partial melt of a K and H_2O-rich mantle source (Stolper et al., 2013). An even more oxidized reservoir in the martian mantle might therefore exist.

6. Conclusions

Estimates of igneous fO_2 for the relatively unaltered Gusev basalts by two different methods (-3.6 to $+0.7$ ΔQFM) are strikingly similar to estimates for the shergottitic meteorites (-3.7 to 0.3 ΔQFM; Goodrich et al., 2003; Herd et al., 2001, 2002; Herd, 2003, 2006; Peslier et al., 2010). Although a few more oxidized exceptions exist among the meteorite dataset (nakhlite MIL 03346 and post-magmatic conditions of basaltic breccia NWA 7034; Dyar et al., 2005; Agee et al., 2013b), they are apparently not analogous to conditions of formation for the Gusev basalts. The overall range in fO_2 in the source mantle for martian basaltic magmas is therefore relatively restricted.

In the Earth, variations in mantle fO_2 are attributed to recycling of oxidized surface material at subduction zones (e.g., Frost and McCammon, 2008). For Mars, the reduced nature of some Gusev basalts and olivine-phyric meteorites provide no evidence for tectonic processes having affected the overall oxidation state of the mantle (Fig. 5). Yet an incompatible element-rich component of the martian interior was involved in the petrogenesis of the K-rich Irvine and Humboldt Peak basalts as well as the LREE-enriched basaltic shergottites. The nature of the oxidized component likely differs for the meteorite and Gusev datasets and may signify tapping of mantle source heterogeneities formed during early differentiation of the planet, metasomatism by oxidizing fluids, or crustal contamination.

Acknowledgements

We are grateful to reviews by Chris Herd and one anonymous reviewer. This work was supported by an NSERC Discovery Grant to M. Schmidt and by a NASA Athena Participating Scientist Grant to T. McCoy. We also acknowledge the MER Science and Engineering Team for their contributions to the success of the mission.

References

Agee, C.B., Wilson, N.V., McCubbin, F.M., Ziegler, K., Polyak, V.J., Sharp, Z.D., Asmerom, Y., Nunn, M.H., Shaheen, R., Thiemens, M.H., Steele, A., Fogel, M.L., Bowden, R., Glamoclija, M., Zhang, Z., Elardo, S.M., 2013a. Unique meteorite from early Amazonian Mars: Water-rich basaltic breccia Northwest Africa 7034. Science 339, 780–785, http://dx.doi.org/10.1126/science.1228858.

Agee, C.B., McCubbin, F.M., Shearer, C.S., Santos, A.R., Burkemper, L.K., Provencio, P., Wilson, N.V., 2013b. Oxide phases and oxygen fugacity of martian basaltic breccia Northwest Africa 7034. Lunar Planet. Sci. Conf. Abstr., 2965.

Arvidson, R.E., et al., 2006. Overview of the Spirit Mars Exploration Rover mission to Gusev Crater: landing site to Backstay rock. J. Geophys. Res. 111, E02S01, http://dx.doi.org/10.1029/2005JE002499.

Blinova, A., Herd, C.D.K., 2009. Experimental study of polybaric REE partitioning between olivine, pyroxene and melt of Yamato 980459 composition: Insights into the petrogenesis of depleted shergottites. Geochim. Cosmochim. Acta 73, 3471–3492.

Borg, L.E., Draper, D.S., 2003. A petrogenetic model for the origin and compositional variation of the martian basaltic meteorites. Meteorit. Planet. Sci. 38, 1713–1731.

Borg, L.E., Nyquist, L.E., Taylor, L.A., Weismann, H., Shih, C.-Y., 1997. Constraints on martian differentiation process from Rb–Sr and Sm–Nd isotopic analyses of the basaltic shergottite QUE 94201. Geochim. Cosmochim. Acta 61, 4915–4931.

Dyar, D., 2003. Ferric iron in SNC meteorites as determined by Mössbauer spectroscopy: Implications for martian landers and martian oxygen fugacity. Meteorit. Planet. Sci. 38, 1733–1752.

Dyar, M.D., Treiman, A.H., Pieters, C.M., Hiroi, T., Lane, M.D., O'Connor, V., 2005. MIL03346, the most oxidized martian meteorite: A first look at spectroscopy, petrography, and mineral chemistry. J. Geophys. Res. 110, E09005, http://dx.doi.org/10.1029/2005JE002426.

Ehlmann, B.L., Mustard, J.F., Murchie, S.L., 2010. Geologic setting of serpentine deposits on Mars. Geophys. Res. Lett. 37, L06201, http://dx.doi.org/10.1029/2010GL042596.

Frost, D.J., McCammon, C.A., 2008. The redox state of the Earth's mantle. Annu. Rev. Earth Planet. Sci. 36, 389–420.

Gellert, R., Reider, R., Brückner, J., Clark, B.C., Dreibus, G., Klingelhöfer, G., Lugmair, G., Ming, D.W., Wänke, H., Yen, A., Zipfel, J., Squyres, S.W., 2006. Alpha Particle X-ray Spectrometer (APXS): results from Gusev Crater and calibration report. J. Geophys. Res. 111, E02S05, http://dx.doi.org/10.1029/2005JE002555.

Goodrich, C.A., Herd, C.D.K., Taylor, L.A., 2003. Spinels and oxygen fugacity in olivine-phyric and lherzolitic shergottites. Meteorit. Planet. Sci. 38, 1773–1792.

Greeley, R., Foing, B.H., McSween, H.Y., Neukum, G., Pinet, P., van Kan, M., Werner, S.W., Williams, D.A., 2005. Fluid lava flows in Gusev Crater. J. Geophys. Res. 110, E05008, http://dx.doi.org/10.1029/2005JE002401.

Gross, J., Treiman, A.H., Filiberto, J., Herd, C.D.K., 2011. Primitive olivine-phyric shergottite NWA 5789: Petrography, mineral chemistry, and cooling history imply a magma similar to Yamato-980459. Meteorit. Planet. Sci. 46, 116–133.

Hauck, S.A., Phillips, R.J., 2002. Thermal and crustal evolution of Mars. J. Geophys. Res. 107, 5052, http://dx.doi.org/10.1029/2001JE001801.

Hausrath, E.M., Navarre-Stichler, A.K., Sak, P.B., Steefel, C.I., Brantley, S.L., 2008. Basalt weathering rates on Earth and the duration of liquid water on the plains of Gusev Crater, Mars. Geology 36, 67–70.

Herd, C.D.K., 2003. The oxygen fugacity of olivine-phyric martian basalts and the components within the mantle and crust of Mars. Meteorit. Planet. Sci. 38, 1793–1805.

Herd, C.D.K., 2004. Oxygen in martian meteorites: a review of results from mineral equilibria oxybarometers. In: Workshop on Oxygen in the Terrestrial Planets. Abs. 3026.

Herd, C.D.K., 2006. Insights into the redox history of NWA 1068/1110 martian basalt from mineral equilibria and vanadium oxybarometry. Am. Mineral. 91, 1616–1627.

Herd, C.D.K., Papike, J.J., Brearley, A.J., 2001. Oxygen fugacity of martian basalts from electron microprobe oxygen and TEM-EELS analyses of Fe–Ti oxides. Am. Mineral. 86, 1015–1024.

Herd, C.D.K., Borg, L.E., Jones, J.H., Papike, J.J., 2002. Oxygen fugacity and geochemical variations in the martian basalts: Implications for martian basalt petrogenesis and the oxidation state of the upper mantle of Mars. Geochim. Cosmochim. Acta 66, 2025–2036.

Holloway, J.R., Pan, V., Gudmundsson, G., 1992. High-pressure fluid-absent melting experiments in the presence of graphite: Oxygen fugacity, ferric/ferrous ratio and dissolved CO_2. Eur. J. Mineral. 4, 105–114.

Hurowitz, J.A., McLennan, S.M., Tosca, N.J., Arvidson, R.E., Michalski, J.R., Ming, D.W., Schröder, C., Squyres, S.W., 2006. In situ and experimental evidence for acidic weathering of rocks and soils on Mars. J. Geophys. Res. 111, E02S19, http://dx.doi.org/10.1029/2005JE002515.

Joliff, B.L., Farrand, W.H., Johnson, J.R., Schröder, C., Weitz, C.M., 2006. Origin of rocks and cobbles on the Meridiani Plains as seen by Opportunity. Lunar Planet. Sci. Conf. Abstr., 2401.

Kelley, K.A., Cottrell, E., 2009. Water and oxidation state of subduction zone magmas. Science 325, 605–607.

Klingelhöfer, G., Morris, R.V., Bernhardt, B., Rodionov, D., de Souza Jr., P.A., Squyres, S.W., Foh, J., Kankeleit, E., Bonnes, U., Gellert, R., Schröder, C., Linkin, S., Evanov, E., Zubkov, B., Prilutski, O., 2003. Athena MIMOS II Mössbauer spectrometer investigation. J. Geophys. Res. 108, 8067, http://dx.doi.org/10.1029/2003JE002138.

Kress, V.C., Carmichael, I.S.E., 1991. The compressibility of silicate liquids containing Fe_2O_3 and the effect of composition, temperature, oxygen fugacity and pressure on their redox states. Contrib. Mineral. Petrol. 108, 82–92.

Lécuyer, C., Ricard, Y., 1999. Long-term fluxes and budget of ferric iron: implication for the redox states of the Earth's mantle and atmosphere. Earth Planet. Sci. Lett. 165, 197–211.

Madsen, M.B., Goetz, W., Bertelsen, P., Binau, C.S., Folkmann, F., Gunnlaugsson, H.P., Hjøllum J, í, Hviid, S.F., Jensen, F., Kinch, K.M., Leer, K., Madsen, D.E., Merrison, J., Olsen, M., Arneson, H.M., Bell III, J.F., Gellert, R., Herkenhoff, K.E., Johnson, J.R., Johnson, M.J., Klingelhöfer, G., McCartney, E., Ming, D.W., Morris, R.V., Proton, J.B., Rodionov, D., Sims, M., Squyres, S.W., Wdowiak, T., Yen, A.S., 2009. Overview of the magnetic properties experiments on the Mars Exploration Rovers. J. Geophys. Res. 114, E06S90, http://dx.doi.org/10.1029/2008JE003098.

McCanta, M.C., Dyar, M.D., Rutherford, M.J., Delaney, J.S., 2004. Iron partitioning between basaltic melts and clinopyroxene as a function of oxygen fugacity. Am. Mineral. 89, 1685–1693.

McCanta, M.C., Elkins-Tanton, L., Rutherford, M.J., 2009. Expanding the application of the Eu-oxybarometer to the lherzolitic shergottites and nakhlites: Implications for the oxidation state heterogeneity of the martian interior. Meteorit. Planet. Sci. 44, 725–745.

McCubbin, R.M., Elardo, S.M., Shearer Jr., C.K., Smirnov, A., Hauri, E.H., Draper, D.S., 2013. A petrogenetic model for the comagmatic origin of chassignites and nakhlites: Inferences from chlorine-rich minerals, petrology, and geochemistry. Meteorit. Planet. Sci. 48, 819–853, http://dx.doi.org/10.1111/maps.12095.

McSween, H.Y., Treiman, A.H., 1998. Martian meteorites. In: Papike, J.J. (Ed.), Planetary Materials. Rev. Mineral. 36, 1–53.

McSween, H.Y., et al., 2004. Basaltic rocks analyzed by the Spirit rover in Gusev Crater. Science 305, 842–845, http://dx.doi.org/10.1126/science.3050842.

McSween, H.Y., et al., 2006a. Characterization and petrologic interpretation of olivine-rich basalts at Gusev Crater, Mars. J. Geophys. Res. 111, E02S10, http://dx.doi.org/10.1029/2005JE002477.

McSween, H.Y., Ruff, S.W., Morris, R.V., Bell III, J.F., Herkenhoff, K., Gellert, R., Stockstill, K.R., Tornabene, L.L., Squyres, S.W., Crisp, J.A., Christensen, P.R., McCoy, T.J., Mittlefehldt, D.W., Schmidt, M., 2006b. Alkaline volcanic rocks from the Columbia Hills, Gusev Crater, Mars. J. Geophys. Res. 111, E09S91, http://dx.doi.org/10.1029/2006JE002698.

McSween, H.Y., Ruff, S.W., Morris, R.V., Gellert, R., Klingelhöfer, G., Christensen, P.R., McCoy, T.J., Ghosh, A., Moersch, J.M., Cohen, B.A., Rogers, A.D., Schröder, C., Squyres, S.W., Crisp, J.A., Yen, A., 2008. Mineralogy of volcanic rocks in Gusev Crater, Mars: reconciling Mössbauer, Alpha Particle X-ray Spectrometer, and Miniature Thermal Emission Spectrometer spectra. J. Geophys. Res. 113, E06S04, http://dx.doi.org/10.1029/2007JE002970.

Meyer, C., 2013. The martian meteorite compendium, astromaterials research and exploration science. http://curator.jsc.nasa.gov/antmet/mmc/index.cfm2013.

Ming, D.W., Gellert, R., Morris, R.V., Arvidson, R.E., Brückner, J., Clark, B.C., Cohen, B.A., d'Uston, C., Economou, T., Fleischer, I., Klingelhöfer, G., McCoy, T.J., Mittlefehldt, D.W., Schmidt, M.E., Schröder, C., Squyres, S.W., Trégiur, E., Yen, A.S., Zipfel, J., 2008. Geochemical properties of rocks and soils in Gusev Crater, Mars: results of the Alpha Particle X-ray Spectrometer from Cumberland Ridge to Home Plate. J. Geophys. Res. 113, E12S39, http://dx.doi.org/10.1029/2008JE003195.

Monders, A.G., Médard, E., Grove, T.L., 2007. Phase equilibrium investigations of the Adirondack class basalts from the Gusev plains, Gusev crater. Meteorit. Planet. Sci. 42, 131–148.

Morris, R.V., Klingelhöfer, G., Schröder, C., Rodionov, D.S., de Souza Jr., P.A., Yen, A., Gellert, R., Evlanov, E.N., Foh, J., Kankeleit, E., Gütlich, P., Ming, D.W., Renz, F., Wdowiak, T., Squyres, S.W., Arvidson, R.E., 2004. Mineralogy at Gusev Crater from the Mössbauer Spectrometer on the Spirit Rover. Science 305, 833–836.

Morris, R.V., Klingelhöfer, G., Schröder, C., Rodionov, D.S., Yen, A., Ming, D.W., de Souza, P.A., Fleischer, I., Wdowiak, T., Gellert, R., Bernhardt, B., Evlanov, E.N., Zubkov, B., Foh, J., Bonnes, U., Kankeleit, E., Gütlich, P., Renz, F., Squyres, S.W., Arvidson, R.E., 2006a. Mössbauer mineralogy of rock, soil, and dust at Gusev crater, Mars: Spirit's journey through weakly altered olivine basalt on the plains and pervasively altered basalt in the Columbia Hills. J. Geophys. Res. 111, E02S13, http://dx.doi.org/10.1029/2005JE002584.

Morris, R.V., Klingelhöfer, G., Schröder, C., Rodionov, D.S., Yen, A., Ming, D.W., de Souza Jr., P.A., Wdowiak, T., Fleischer, I., Gellert, R., Bernhardt, B., Bonnes, U., Cohen, B.A., Evlanov, E.N., Foh, J., Gütlich, P., Kankeleit, E., McCoy, T., Mittlefehldt, D.W., Renz, R., Schmidt, M.E., Zubkov, B., Squyres, S.W., Arvidson, R.E., 2006b. Mössbauer mineralogy of rock, soil, and dust at Meridiani Planum, Mars: Opportunity's journey across sulfate-rich outcrop, basaltic sand and dust, and hematite lag deposits. J. Geophys. Res. 111, E12S15, http://dx.doi.org/10.1029/2006JE002791.

Morris, R.V., Klingelhöfer, G., Schröder, C., Fleischer, I., Ming, D.W., Yen, A.S., Gellert, R., Arvidson, R.E., Rodionov, D.S., Crumpler, L.S., Clark, B.C., Cohen, B.A., McCoy, T.J., Mittlefehldt, D.W., Schmidt, M.E., de Souza Jr., P.A., Squyres, S.W.,

2008. Iron mineralogy and aqueous alteration from Husband Hill through Home Plate at Gusev Crater, Mars: results from the Mössbauer instrument on the Spirit Mars Exploration Rover. J. Geophys. Res. 113, E12S42, http://dx.doi.org/10.1029/2008JE003201.

Parkinson, I.J., Arculus, R.J., 1999. The redox state of subduction zones: insights from arc-peridotites. Chem. Geol. 160, 409–423.

Peslier, A.H., Hnatyshin, D., Herd, C.D.K., Walton, E.L., Brandon, A.D., Lapen, T.J., Shafer, J.T., 2010. Crystallization, melt inclusion, and redox history of a martian meteorite: Olivine-phyric shergottite Larkman Nunatak 06319. Geochim. Cosmochim. Acta 74, 4543–4576.

Rieder, R., Gellert, R., Brückner, J., Klingelhöfer, G., Dreibus, G., Yen, A., Squyres, S.W., 2003. The new Athena Alpha Particle X-Ray Spectrometer (APXS) for the Mars Exploration Rovers. J. Geophys. Res. 108, 8066, http://dx.doi.org/10.1029/2003JE002150.

Rieder, R., Gellert, R., Anderson, R.C., Brückner, J., Clark, B.C., Dreibus, G., Economou, T., Klingelhöfer, G., Lugmair, G.W., Ming, D.W., Squyres, S.W., d'Uston, C., Wänke, H., Yen, A., Zipfel, J., 2004. Chemistry of rocks and soils at Meridiani Planum from the Alpha Particle X-ray Spectrometer. Science 306, 1746, http://dx.doi.org/10.1126/science.1104358.

Ruedas, T., Tackley, P.J., Solomon, S.C., 2013. Thermal and compositional evolution of the martian mantle: Effects of phase trasitions and melting. Phys. Earth Planet. Inter. 216, 32–58, http://dx.doi.org/10.1016/j.pepi2012.12.002.

Sato, M., 1978. Oxygen fugacity of basaltic magmas and the role of gas-forming elements. Geophys. Res. Lett. 5, 447–449, http://dx.doi.org/10.1029/GL005i006p00447.

Sato, M., Hickling, N.L., McLane, J.E., 1973. Oxygen fugacity values of Apollo 12, 14, and 15 lunar samples and reduced state of lunar magmas. In: Proc. 4th Lunar Sci. Conf., vol. 1, pp. 1061–1079.

Schmidt, M.E., McCoy, T.J., 2010. The evolution of a heterogeneous martian mantle: Clues from K, P, Ti, Cr, and Ni variations in Gusev basalts and shergottite meteorites. Earth Planet. Sci. Lett. 296, 67–77, http://dx.doi.org/10.1016/j.epsl.2010.04.046.

Schmidt, M.E., Ruff, S.W., McCoy, T.J., Farrand, W.H., Johnson, J.R., Gellert, R., Ming, D.W., Morris, R.V., Cabrol, N., Lewis, K.W., Schroeder, C., 2008. Hydrothermal origin of halogens at Home Plate, Gusev Crater. J. Geophys. Res. 113, E06S12, http://dx.doi.org/10.1029/2007JE003027.

Schmidt, M.E., Farrand, W.H., Johnson, J.R., Schröder, C., Hurowitz, J.A., McCoy, T.J., Ruff, S.W., Arvidson, R.E., Des Marais, D.J., Lewis, K.W., Ming, D.W., Squyres, S.W., de Souza Jr., P.A., 2009. Spectral, mineralogical, and geochemical variations across Home Plate, Gusev Crater, Mars indicate high and low temperature alteration. Earth Planet. Sci. Lett. 281, 258–266.

Shearer, C.K., Burger, P.V., Sutton, S.R., Papike, J.J., McCubbin, F., 2011. REE crystal chemistry of phosphates in extraterrestrial basalts at different oxygen fugacities: Direct determination of europium valence state in merrillite–whitlockite. Lunar Planet. Sci. 42. Abs. 1143.

Stolper, E.M., Baker, M.B., Newcombe, M.E., Schmidt, M.E., Treiman, A.H., Cousin, A., Dyar, M.D., Fisk, M.R., Gellert, R., King, P.L., Leshin, L., Maurice, S., McLennan, S.M., Minitti, M.E., Perrett, G., Rowland, S., Sautter, V., Wiens, R.C., MSL Science Team, 2013. The petrochemistry of Jake_M: A martian mugearite. Science 341, http://dx.doi.org/10.1126/science.1239463.

Sun, S.-s, McDonough, W.F., 1989. Chemical and isotopic systematics of oceanic basalts: implications for mantle composition and processes. Geol. Soc. Lond. Special Pub. 42, 313–345, http://dx.doi.org/10.1144/GSL.SP.1989.04.01.19.

Szymanski, A., Brenker, F.E., Palme, H., El Goresy, A., 2010. High oxidation state during formation of martian nakhlites. Meteorit. Planet. Sci. 45, 21–31.

Toplis, M.J., Carroll, M.R., 1996. Differentiation of ferro-basaltic magmas under conditions open and closed to oxygen: Implications for the Skaergaard Intrusion and other natural systems. J. Petrol. 37, 837–858.

Tosca, N.J., McLennan, S.M., Lindsley, D.H., Schoonen, M.A.A., 2004. Acid-sulfate weathering of synthetic martian basalt: The acid fog model revisited. J. Geophys. Res. 109, E05003, http://dx.doi.org/10.1029/2003JE002218.

Treiman, A.H., 2003. Chemical compositions of martian basalts (shergottites): Some inferences on basalt formation, mantle metasomatism, and differentiation in Mars. Meteorit. Planet. Sci. 38, 1849–1864.

Tuff, J., Wade, J., Wood, B.J., 2013. Volcanism on Mars controlled by early oxidation of the upper mantle. Nature 498, 342–345.

Wadhwa, M., 2001. Redox state of Mars' upper mantle and crust from Eu anomalies in shergottite pyroxenes. Science 291, 1527–1530.

Wänke, H., Dreibus, G., 1988. Chemical composition and accretion history of terrestrial planets. Philos. Trans. R. Soc. Lond. 325, 545–557.

Wones, D.R., Gilbert, M.C., 1969. The fayalite-magnetite-quartz assemblage between 600 and 800 °C. Am. J. Sci. 267, 480–488.

Wood, B.J., 1991. Oxygen barometry of spinel peridotites. Rev. Mineral. Geochem. 25, 417–431.

Zipfel, J., Schröder, C., Joliff, B.L., Gellert, R., Herkenhoff, K.E., Rieder, R., Anderson, R., Bell III, J.F., Brückner, J., Crisp, J.A., Christensen, P.R., Clark, B.C., de Souza Jr., P.A., Dreibus, G., D'Uston, C., Economou, T., Gorevan, S.P., Hahn, B.C., Klingelhöfer, G., McCoy, T.J., McSween, H.Y., Ming, D.W., Morris, R.V., Rodionov, D.S., Sqyres, S.W., Wänke, H., Wright, S.P., Wyatt, M.B., Yen, A.S., 2011. Bounce Rock – A shergottite-like basalt encountered in Meridiani Planum, Mars. Meteorit. Planet. Sci. 46, 1–20.